Cell Shape and Interaction Defects in α-Spectrin Mutants of *Drosophila Melanogaster*

John K. Lee, Robert S. Coyne, Ronald R. Dubreuil, Lawrence S. B. Goldstein, and Daniel Branton

Department of Cellular and Developmental Biology, Harvard University, Cambridge, Massachusetts 02138

Abstract. We show that the α-spectrin gene is essential for larval survival and development by characterizing several α-spectrin mutations in *Drosophila*. P-element minigene rescue and sequence analysis were used to identify the α-spectrin gene as the *l(3)dre3* complementation group of the *Dras-Roughened-ecdysoneless* region of chromosome 3 (Sliter et al., 1988). Germ line transformants carrying an α-spectrin cDNA, whose expression is driven by the ubiquitin promoter, fully rescued the first to second instar lethality characteristic of the *l(3)dre3* alleles. The molecular defects in two γ-ray–induced alleles were identified. One of these mutations, which resulted in second instar lethality, contained a 37-bp deletion in α-spectrin segment 22 (starting at amino acid residue 2312), producing a premature stop codon between the two EF hands found in this segment. The second mutation, which resulted in first instar lethality, contained a 20 base pair deletion in the middle of segment 1 (at amino acid residue 92), resulting in a premature stop codon. Examination of the spectrin-deficient larvae revealed a loss of contact between epithelial cells of the gut and disruption of cell–substratum interactions. The most pronounced morphological change was seen in tissues of complex cellular architecture such as the middle midgut where a loss of cell contact between cup-shaped cuprophilic cells and neighboring interstitial cells was accompanied by disorganization of the cuprophilic cell brush borders. Our examination of spectrin deficient larvae suggests that an important role of non-erythroid spectrin is to stabilize cell to cell interactions that are critical for the maintenance of cell shape and subcellular organization within tissues.

PHENOTYPIC analyses of spectrin deficiencies in mice and humans have provided strong evidence that the spectrin-based membrane skeleton of the erythrocyte contributes to the long range order and stability of the plasma membrane by enhancing mechanical integrity and deformability (Davies and Lux, 1989; Palek and Lambert, 1990). Despite a number of similarities in the structural properties of erythroid and non-erythroid spectrins, significant differences between the two suggest that non-erythroid spectrins may perform functions that are not predicted by the red blood cell model. In non-erythroid cells spectrin can and does interact with a far greater variety of proteins than exists in the erythrocyte (for a review see Bennett, 1990). Furthermore, non-erythroid spectrin is not confined to simply maintaining static membrane skeletal networks. Non-erythroid spectrins have been observed to undergo spatial reorganization from cytoplasmic stores to regions of high plasma membrane activity in activated lymphocytes (Lee et al., 1988*b*), in membrane furrows of *Drosophila* embryos (Pesacreta et al., 1989) and in secreting rat parietal cells (Mercier et al., 1989). In addition, spectrin undergoes cycles of solubility and phosphorylation coincident with mitosis in tissue culture cells (Fowler and Adam, 1992) and cell to cell contact in MDCK cells (Nelson and Veshnock, 1987; Morrow et al., 1989). These observations suggest that nonerythroid spectrin serves multiple roles by providing stable linkages to establish membrane domains and exists in reservoirs capable of rapid assembly and disassembly in response to changes in metabolic activity.

In one approach to elucidate the functions of non-erythroid α-spectrin, Mangeat and Burridge (1984) injected anti-α-spectrin antibodies into cells grown in vitro. Microinjection of purified α-spectrin antibodies into a variety of tissue culture cells visibly aggregated spectrin but did not perturb the overall cell shape, integrity of microfilament bundles, or cell viability. Rather, injection of anti-spectrin

Please address all correspondence to Dr. Branton, Department of Cellular and Developmental Biology, Harvard University, 16 Divinity Ave., Cambridge, MA 02138.

Dr. Coyne's present address is Fred Hutchinson Cancer Center, M/385, 1124 Columbia Street, Seattle, WA 98104.

Dr. Dubreuil's present address is Department of Pharmacology and Physiological Science, University of Chicago, 947 E. 58th Street, Box 271, Chicago, IL 60637.

antibody caused only the collapse of the intermediate filament network. While these results are hard to interpret, the in vitro cultured environment may not have required those spectrin dependent cellular activities that are manifested during changes in cell morphology or viability. We have therefore undertaken mutational analysis in *Drosophila* to evaluate the in vivo requirement for spectrin in fly development and intracellular organization.

Drosophila α-spectrin is similar to the vertebrate form in sequence (Dubreuil et al., 1989), subunit structure, capacity to cross-link F-actin (Dubreuil et al., 1987) and cellular localization in embryos (Pesacreta et al., 1989). The *Drosophila* α-spectrin gene is located in the *Dras-Roughened-ecdysoneless* (*DRE*)[1] region of chromosome 3 (Byers et al., 1987 and Coyne, 1989), which has been mutagenized to saturation (Sliter et al., 1989). Here we show that the *l(3)dre3* complementation group in the first interval of the *DRE* region of chromosome 3 consists of mutations in α-spectrin. Analysis of the mutant alleles in this complementation group demonstrates that α-spectrin is essential for the viability of *Drosophila*. Furthermore, a depletion of α-spectrin leads to the loss of cell to cell contact, formation of abnormally shaped cells in the digestive system and death at first or second instar of larval development.

Materials and Methods

Fly Stocks and Culture Conditions

Alleles of the original *dre* complementation groups and the *R* and *G* series deficiencies were obtained from L. Gilbert (University of North Carolina at Chapel Hill, and see Sliter et al., 1989). The alleles of the *l(3)dre3* complementation group used in this study are; $l(3)dre3^{lm32}$, $l(3)dre3^{rg35}$, $l(3)dre3^{rg41}$, $l(3)dre3^{lm88}$, $l(3)dre3^{lm102}$, and $l(3)dre3^{lm111}$. One other member of the *dre3* group, $l(3)dre3^{lm73}$, was not available at the time of the study. Alleles of the other complementation groups used in this study are as follows, for *l(3)dre9*: $l(3)dre9^{lm58}$ and $l(3)dre9^{lm84}$; for *l(3)drel*: $l(3)drel^{lm31}$ and $l(3)drel^{lm84}$; for *l(3)dre2*: $l(3)dre2^{rg17}$ and $l(3)dre2^{lm118}$; and for *l(3)neo7*: *l(3)neo7*. The third chromosome balancer marked with *yellow*$^+$, *(In(3LR)TM3, y*$^+$*Sb Ser)* was kindly provided by E. Fyrberg (Johns Hopkins University, Baltimore, MD), and the Δ2-3 transposase stock (ry^{506} P[ry^+ *Δ2-3]99B*), by W. Engels (University of Wisconsin, Madison, WI; and see Robertson et al., 1988). Unless otherwise noted, mutations and chromosomes used in this study are described in Lindsley and Zimm (1992). Stocks were maintained on a standard molasses-cornmeal-yeast-agar medium. Embryos and larvae were collected at 25°C on grape juice-agar plates supplemented with yeast paste.

Isolation of cDNA and Genomic Clones

Isolation of cDNA clones 9 and 10 was described (Byers et al., 1987). A 3.8-kb EcoRI fragment of clone 9 inserted into pBluescript-SK, (referred to as pBS 9-1; Fig. 1 *a*), was used to screen a λ genomic library. This library (obtained from R. Blackman, Harvard University, Boston, MA) was constructed by insertion of size-selected DNA fragments into the BamHI site of λEMBL3. Approximately 72,000 plaques were screened and 59 hybridizing plaques were initially detected. Ten of the positive phage were purified to homogeneity and DNA prepared from five was digested with SalI. Three clones (λsp5f, λsp3a, and λsp3e; Fig. 1 *a*) were selected based on their distinctive SalI digestion patterns and were further restriction mapped.

Transformation Rescue of α-Spectrin Mutants

Insertion of the α-spectrin minigene into the P-element transformation vector, pW8, is detailed in the results section. Germ line transformants were generated according to Spradling and Rubin (1982); embryos were collected at 25°C and dechorionated in 50% bleach and desiccated. CsCl-purified DNA was prepared in 5 mM KCl, 0.1 mM $NaPO_4$, pH 6.8, and injected into Δ2-3 embryos (Robertson et al., 1988) to produce stable transformants. Embryos were allowed to develop at room temperature until hatching at which time they were transferred to standard food at 25°C. Enclosed adults were mated to the yw^{67c23} stock to screen for positive transformants. Of the positive transformants, two independent insertions that mapped to the X chromosome, as judged by segregation patterns, were used in the rescue crosses.

Fixation of Larvae and Antibody Staining

Rabbit antibody 354 generated against a recombinant fragment of *Drosophila* α-spectrin (encompassing segments 11-21) was used for all immunofluorescence and immunoblot experiments. The serum, used at dilutions of 1:2,500 for immunofluorescence and 1:5,000 for immunoblots, was previously characterized (referred to as antibody 905 in Byers et al., 1987; and Pesacreta et al., 1989). Monoclonal antibody 4A1 (Theurkauf, 1992) was used for α-tubulin detection. TRITC-phalloidin from Molecular Probes (Eugene, OR) was used for F-actin localization. The monoclonal antibody α5 (kindly provided by M. Caplan, Yale University, New Haven, CT) was used to detect a *Drosophila* isoform of the α-subunit of Na^+,K^+-ATPase (Lebovitz et al., 1989). For whole-mount staining of larval tissues, mutant, and wild-type animals (as identified by the method detailed below) were dissected in 2% formaldehyde in PBS and fixed for an additional 15 min. Tissues were subsequently washed in PBS supplemented with 50 mM NH_4Cl for 15 min followed by a rinse in PBS. Before the addition of antisera, tissues were incubated in blocking buffer (PBS with 2% newborn calf serum and 0.5% Triton X-100) for 30 min. After incubation with the appropriate primary antisera, samples were washed and incubated in FITC-conjugated anti-IgG antiserum (Zymed, San Francisco, CA). For double labeling, a Texas red secondary reagent (Southern Biotechnology, Birmingham, AL) was used in combination with the FITC label. Images were collected on a MRC-600 scanning confocal microscope (Bio-Rad, Cambridge, MA). Fixation and sectioning of midgut tissues for ultrastructural analysis were performed as described (Filshie et al., 1971).

Immunoblot Analysis

Individual first instar larvae were selected from crosses between the mutant alleles maintained over the third chromosome balancer marked with *yellow*$^+$, (yw^{67c23}; *ru l(3)dre*^{x} *st e/In(3LR)TM3, y*$^+$ *Sb Ser*) and the similarly balanced *R-R2* deficiency (yw^{67c23}; *Df(3L)R-R2,ve/TM3, y*$^+$ *Sb Ser*). Upon mating, females were allowed to lay eggs on standard grape plates at 25°C. Hemizygous mutant larvae were distinguished from larvae containing the *TM3* third chromosome balancer marked with *yellow*$^+$ (and carrying a wild-type copy of the α-spectrin gene) based on their mouthhook color, which is affected by the *yellow* mutation (Brehme, 1941). (The balancer chromosome contributes a *yellow*$^+$ phenotype that is distinguishable from hemizygous mutant larvae lacking the balancer chromosome.) Each larva was individually homogenized and solubilized in standard Laemmli sample buffer. The entire volume was electrophoresed in one lane of an 8% SDS-PAGE gel (Laemmli, 1970), transferred to nitrocellulose, and immunostained according to a modification (Dubreuil et al., 1987) of a previously described protocol (Burnette, 1981).

Polymerase Chain Reaction and Sequencing

Polymerase chain reactions (PCR) were done according to Saiki et al. (1988). Sequencing of PCR fragments was carried out as described by Casanova et al. (1990) with the following modifications: template DNA was isolated using Geneclean (Bio101, Vista, CA) and added to the sequencing reaction at a primer/template ratio of 100:1. Sequenase 2.0 from United States Biochemical Corp. (Cleveland, OH) was used for sequencing reactions.

Southern Blot Analysis

Genomic DNA from single flies was prepared according to Simon et al. (1985), digested with restriction enzyme, and then loaded onto 0.7% agarose gels. After electrophoresis, nucleic acids were transferred onto Zetaprobe membranes (Bio-Rad, Rockville Center, NY) using the alkali blotting method (Reed and Mann, 1985) and hybridized by the method of

1. *Abbreviations used in this paper*: EMS, ethane methyl sulfonate; DRE, Dras-Roughened-ecdysoneless; PCR, polymerase chain reaction.

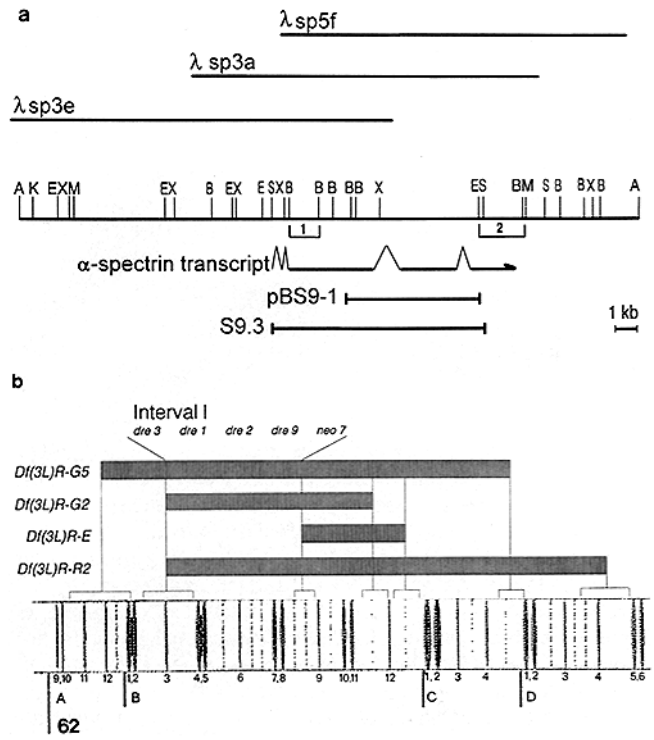

Figure 1. (*a*) Restriction map of α-spectrin genomic DNA. The upper three lines show the relative length and regions of overlap of the λ clones (*sp5f, sp3a*, and *sp3e*) isolated from a genomic library in λEMBL3; below these lines, a composite genomic restriction map constructed from the maps of the individual λ clones. The bracketed regions identify the termini of the α-spectrin transcript based on hybridization of cDNA fragments to the λ clones. Abbreviations for restriction enzymes: *A*, ApaI; *K*, KpnI; *E* EcoRI; *X*, XhoI; *M*, SmaI; *B*, BamHI; *S*, SalI. Below the composite map is the predicted α-spectrin exon/intron structure, the region included in pBS9-1, and the genomic region (S9.3) used as a probe in the Southern blot (see Fig. 5). (*b*) Cytogenetic map of the *DRE* region. Grey, horizontal bars delineate the extent of the deficiencies used in the mapping experiments. Brackets above the cartoon of the corresponding region of a *Drosophila* salivary gland chromosome, depicting the region 62A-D, indicate regions of uncertainty for each deficiency. Interval I contains the complementation groups examined in this study.

Church and Gilbert (1984). For probe preparation, restriction fragments from genomic subclones were isolated from NuSieve GTG agarose gels (FMC, Rockland, ME) and ^{32}P labeled by random oligonucleotide priming (Feinberg and Vogelstein, 1983).

Results

Genomic Localization and Structure of the α-Spectrin Gene

To identify mutations in α-spectrin, it was necessary first to characterize the organization of the α-spectrin gene. The 3.8-kb Eco RI fragment of λ9 (pBS9–1; see Fig. 1*a*) was used to select clones from a λ phage genomic library containing DNA from a 2nd chromosome isogenic stock of *dp cn bw* flies. The three clones showing distinctive SalI digestion patterns, λsp5f, λsp3a, and λsp3e, defined the composite restriction map shown in Fig. 1 *a*. Comparing the restriction maps of the cDNA (Dubreuil et al., 1989) and genomic clones, it was anticipated that the 5′ end of the α-spectrin cDNA clones (which are full-length with respect to protein-coding sequence) was in close proximity to the 5′ end of the λsp5f clone, and the 3′ end of the transcript was just downstream of the EcoRI-SalI sites in λsp5f. As confirmation, the λ clones were analyzed by hybridization using fragments of the 5′ and 3′ ends of the cDNA sequence as probes. A 1.2-kb EcoRI-BamHI fragment from the 5′ end of the cDNA clone, λ10 (Byers et al., 1987), hybridized to the 1.6-kb BamHI-BamHI fragment in λsp3a (denoted by bracket 1 in Fig. 1 *a*; data not shown). Similarly, a 1.1-kb EcoRI fragment from the 3′ end of clone 9 (Byers et al., 1987) hybridized to the 1.8-kb EcoRI-BamHI fragment of λsp5f (denoted by bracket 2). Analysis of the restriction maps of cDNA and genomic clones in conjunction with sequence data of intron junctions (for details see Coyne, 1989) suggested the primary transcript structure shown in Fig. 1 *a*.

To facilitate the mutational analysis of the α-spectrin gene a series of cytologically visible deficiencies in the 62B region of chromosome 3 (Fig. 1 *b*) was used to refine the position of α-spectrin which was originally mapped to 62B1-7 by Byers et al. (1987). By in situ hybridization, using pBS9.1 as a probe, we placed the α-spectrin gene within the deficiency *Df(3L)R-R2* but distal to *Df(3L)R-E* (data not shown). This localized the gene within the first of five intervals of the (*DRE*) region as defined by the deficiency *Df(3L)R-R2* and its overlap with the other deficiencies (Fig. 1 *b*; Sliter et al., 1989). Previous mutageneses generated one P-element–induced, 48 ethane methyl sulfonate (EMS)-induced and 69 γ-ray–induced lethal mutations in the region defined by *Df(3L)R-R2* (Cooley et al., 1988; and Sliter et al., 1988). Complementation analysis placed the mutations into thirteen complementation groups of which five fall into the subdivision to which α-spectrin maps (interval I). These five complementation groups are designated *l(3)dre3, l(3)drel, l(3)dre2, l(3)dre9,* and *l(3)neo7* (Fig. 1 *b*); they contain seven, three, three, three, and two alleles, respectively.

Identification of α-Spectrin Mutations by Minigene Rescue

We used transformed fly stocks expressing wild-type α-spectrin on the X chromosome to determine which complementation group contains mutations in the α-spectrin gene. The spectrin minigene rescue element was constructed by ligating a full-length α-spectrin cDNA, N8 (which encodes an authentic size polypeptide by in vitro transcription and translation; not shown), to the *Drosophila* ubiquitin promoter (Lee et al., 1988*a*). NcoI restriction sites were introduced at the start codon of both the ubiquitin promoter and the spectrin cDNA to preserve the authentic translation product. This construct was inserted into the polylinker of pW8 (Klemenz et al., 1987), a transformation vector marked with the wild-type gene for *white* and flanked by *P* element termini, give rise to the transposon, *P[w⁺UPS]* (Fig. 2). To test their ability to rescue α-spectrin mutations, two independent germ line transformants carrying P[*w⁺UPS*] were used in crosses with representative alleles of the 5 complementation groups in interval I (listed in materials and methods). All of the *l(3)dre3* alleles tested (*l(3)dre3*^{lm32}, *l(3)dre3*^{rg35}, *l(3)dre3*^{rg41}, *l(3)dre3*^{lm88}, *l(3)dre3*^{lm102}, and

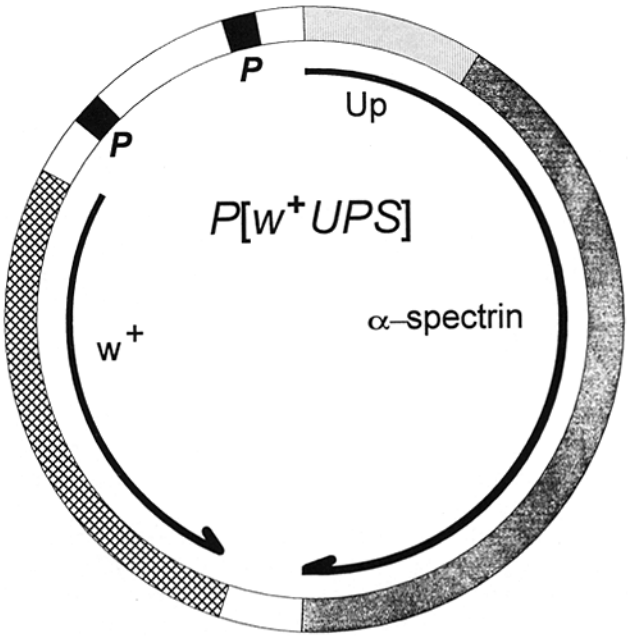

Figure 2. The α-spectrin minigene used to identify spectrin mutations. α-spectrin cDNA (*dark grey region*) was ligated to the *Drosophila* ubiquitin promoter (*light grey region, Up*) using the NcoI restriction site. This product was inserted into the pW8 transformation vector, which is marked with the *white*$^+$ gene (*cross-hatched region, w*$^+$) for selection of transformants and includes two P element repeats (*black region, P*) to create *P[w*$^+$*UPS]*.

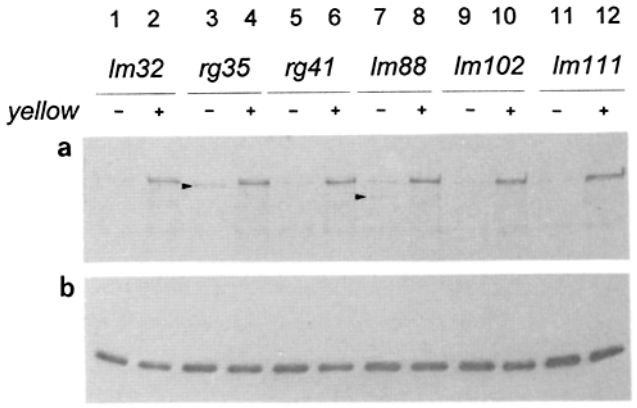

Figure 3. Immunoblot analysis of *dre 3* alleles (see Materials-Fly stocks). Each of the balanced *dre* alleles, {*y w; l(3)dre3/In(3LR)-TM3, y*$^+$ *Sb Ser*} were crossed with the balanced deficiency stock, {*y w;Df(3L)R-R2,ve/In(3LR)TM3, y*$^+$ *Sb Ser*}. Pairs of resultant larvae, one y^- and the other y^+, representing the hemizygous mutant {*l(3)dre3/D(3L)R-R2, ve*} and balanced stock, {*l(3)dre3* or *Df(3L)-R-R2,ve/TM3, y*$^+$ *Sb Ser*} respectively, were selected (based on mouthhook phenotype of *yellow*, see Materials and Methods) homogenized, solubilized, and electrophoresed on 8% Laemmli SDS gels. The blot was cut horizontally at the 97-kD molecular weight marker. (*a*) The upper half blot was probed for α-spectrin with antibody 354; (*b*) the lower half blot was probed for α-tubulin with antibody 4A1 to control for relative loading. y^- larvae are in odd numbered lanes; y^+ in even numbered lanes. Arrowheads in lanes *3* and *7* identify cross-reactive polypeptides that migrate faster than the wild-type product.

l(3)dre3^{lm111}) were rescued to the adult stage by both of the minigene transformants. In contrast, the α-spectrin minigene had no effect on the lethal phase of representative alleles of the other four complementation groups. These results indicated that the *l(3)dre3* group represents mutations in α-spectrin and, based on their first to second instar lethality, that α-spectrin is essential for larval development.

Western Analysis of l(3)dre3 Alleles

As an independent means of identifying α-spectrin alleles, the expression of α-spectrin in representative samples of interval I complementation groups was examined in western blots of individual larvae that were stained with an α-spectrin antibody. To accurately distinguish hemizygous mutants from balanced heterozygotes, larvae were scored based on the lack of the wild-type *yellow* marker which is contributed by the third chromosome balancer (see Materials and Methods). Corroborating the results from the minigene rescue experiments, the hemizygous mutant *l(3)dre3* alleles had greatly reduced levels of α-spectrin relative to wild-type and in two cases contained cross-reactive bands of greater mobility (Fig. 3). Alleles from each of the other four complementation groups of interval I had normal levels of α-spectrin (data not shown). Of the *l(3)dre3* alleles, larvae hemizygous for *l(3)dre3*^{lm32}, *l(3)dre3*^{rg41}, *l(3)dre3*^{lm102}, and *l(3)dre3*^{lm111} showed barely detectable levels of α-spectrin (Fig. 3, lanes *1, 5, 9,* and *11*), suggesting that these alleles represent hypomorphic mutations. Alternatively, these alleles could be null mutations that still retained detectable amounts of maternal α-spectrin (Pesacreta et al., 1989). *l(3)dre3*^{rg35} contained a prominent cross-reactive product migrating at a position approximately 10,000 D smaller than the wild-type product (Fig. 3, lane *3, arrowhead*). The relative intensities of the wild-type spectrin (presumably maternally contributed) compared to the truncated product varied depending on the age of the hemizygous larvae. Wild-type product was most evident at the earliest stages of larval development, whereas the truncated product was more prominent in animals close to death, when wild-type product was virtually undetectable (data not shown). Heterozygous larvae (*l(3)dre3*^{rg35} over the third chromosome balancer) consistently showed a combination of the two products. Finally, *l(3)dre3*^{lm88} displayed a truncated reaction product that co-migrated with the myosin standard (Fig. 3, lane *7, arrowhead*) in addition to the full-length product, presumably of maternal origin. The truncated products in *l(3)dre3*^{rg35} and *l(3)dre3*^{lm88} could be the result of a missense mutation that affects protein stability, or a nonsense mutation that causes premature termination. To discriminate between these two possibilities, we characterized two mutants at the DNA level by sequence analysis of PCR-amplified genomic DNA fragments.

Molecular Analysis of the α-Spectrin Mutants

We selected *l(3)dre3*^{rg35} and *l(3)dre3*^{rg41} for further analysis because we thought that these two γ-ray–induced alleles were likely to contain small deletions that might be readily detected by gel electrophoresis when regions of the mutant genes were compared to wild-type DNA. DNA from homozygous mutant flies carrying the spectrin minigene (*P[w*$^+$*UPS];l(3)dre3*^{rg35}/*l(3)dre3*^{rg35}) was amplified by PCR. The same was done for flies homozygous for P[*w*$^+$*UPS*];

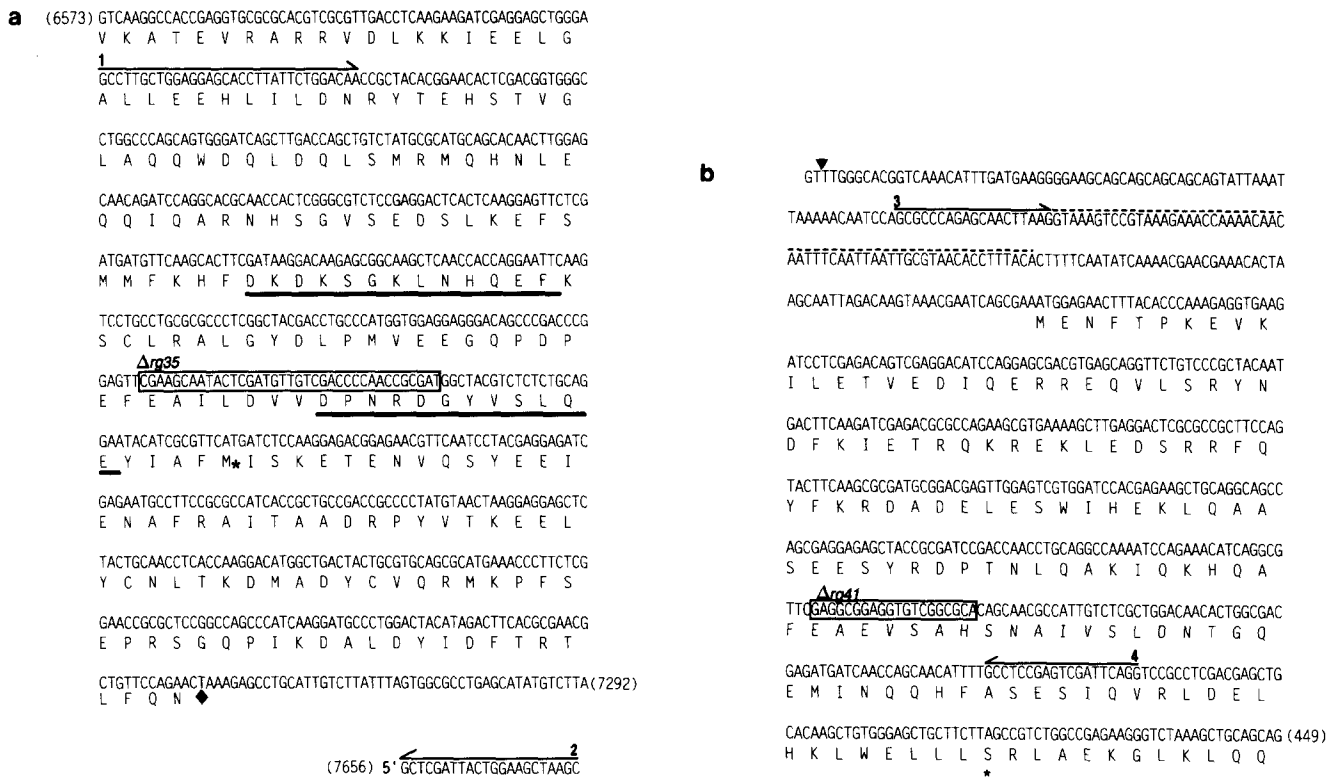

Figure 4. Nucleotide and predicted amino acid sequences in the γ-ray induced dre 3 alleles. (*a*) DNA fragments amplified from the 3′ end of genomic *l(3)dre3*^{rg35} DNA demonstrate a 37-bp deletion (*box*) that results in a frame shift and termination 11-amino acids downstream from the deleted sequence (*asterisk*). This alteration results in a truncation of the last 90 amino acids (a loss of ca. 10,000 D). The underlined residues are the two EF hand consensus sequences in α-spectrin; the diamond indicates the stop codon of the wild type transcript. (*b*) In *l(3)dre3*^{rg41}, a 20-bp deletion (denoted by the box) creates a frameshift and premature termination (*asterisk*). The calculated molecular mass for the resultant 115-amino acid residues is ca. 13,000 D. The dashed line denotes nucleotide sequences of one of two introns that have been mapped to the 5′ untranslated region. The other intron, whose sequence is not shown, is located at the position of the arrowhead. To confirm the deletions read in these sequences, PCR reactions were repeated on genomic DNA from flies rescued by two distinct spectrin minigene insertions. Arrows indicate the oligonucleotide sequences used to prime the PCR products that span the regions of deletion. To design a suitable 3′ antisense primer (2), additional sequences were obtained in the 3′ untranslated region, using the 1.7-kb SalI to BamHI fragment of the λ clone sp5f as a template (Fig. 1). Additional nucleotides were sequenced, from which an antisense primer whose 5′ end begins at nucleotide number 7656 (according to the length of the open reading frame that encodes α-spectrin; Dubreuil et al., 1989) was used in the PCR reactions. The numbers in parentheses at the ends of both sequences (*a* and *b*) indicate the nucleotide number at these positions.

l(3)dre3^{rg41}. To insure that amplification occurred from the endogenous genomic sequences while avoiding priming within the integrated wild-type cDNA sequence, primers complementary to both 5′ and 3′ untranslated regions not contained in P[*w*$^{+}$*UPS*] were used in combination with primers to coding sequences (Fig. 4, *overhead arrows*).

Amplified fragments from the rescued mutant stocks were electrophoresed next to amplified DNA from control stocks bearing P[*w*$^{+}$*UPS*] but otherwise wild type. Fragments with altered mobility were detected toward the 5′ end of the *l(3)dre3*^{rg41} allele and near the 3′ end of the *l(3)dre3*^{rg35} allele (data not shown), and these fragments were sequenced. The altered mobilities of these fragments were found to be due to small deletions in their sequence. *l(3)dre3*^{rg35} contained a deletion of 37 bp near its 3′ terminus (Fig. 4 *a*, *box*) resulting in a termination codon 11 amino acids downstream from the deleted sequence (Fig. 4 *a*, *asterisk*). This alteration results in a truncation of the last 90 amino acids (a calculated loss in mass of 10,000 D) which eliminates the second of two calcium-binding EF hands that have been mapped to this region of *Drosophila* α-spectrin (underlined amino acid residues, Fig. 4 *a*; and Dubreuil et al., 1991). *l(3)dre3*^{rg41} contained a 20-bp deletion (Fig. 4 *b*, *box*) that introduces a premature amber stop codon (*asterisk*) near the 5′ end of the transcript. The calculated molecular mass for the resultant 115 amino acids that might be synthesized is ca. 13,000 D and represents the NH_2-terminal partial repeat (segment 0) and a portion of segment 1 that includes only one of the three α-helices found in the segment (see Winograd et al., 1991; and Byers et al., 1992 for segment phasing). A polypeptide of this molecular mass was not recognized in western blots of *l(3)dre3*^{rg41} larvae stained with antisera 354. This result was not unexpected since the fragment of spectrin would be extremely susceptible to proteolysis (Winograd et al., 1991) and the antisera was made against a fusion polypeptide (clone 9a, see Materials and Methods) encompassing segments 11-21.

Since the *l(3)dre3*^{rg35} deletion eliminated a SalI recognition site, we performed a Southern blot of SalI-digested *l(3)dre3*^{rg35}*/TM6B* DNA (Fig. 5) to verify the sequence of

the PCR product. XhoI and SalI-digested DNA from adult flies was blotted and probed with a genomic fragment (*S9.3*, Fig. 1 *a*). Digested DNA of the heterozygous *l(3)dre3*^{rg35} stock (*l(3)dre3*^{rg35}*/TM6B*) shows two bands, one at the wild-type size (9.8 kb) and the other at a size expected of DNA missing the *l(3)dre3*^{rg35} SalI site (12.5 kb, *arrow*), thus confirming the sequence of the PCR fragment. As a control, the SalI site in *l(3)dre3*^{rg41} genomic DNA was not affected.

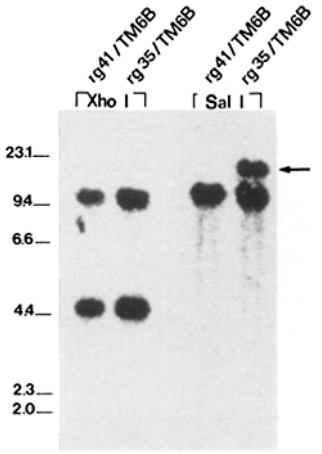

Figure 5. Southern blot analysis of the *l(3)dre3*^{rg35} allele flies. Total DNA from adult flies (*l(3)dre*^{rg41}*/TM6B* or *l(3)dre3*^{rg35}*/TM6B*) was digested with XhoI or SalI (as indicated) and probed with a cloned genomic fragment (S9.3, see Fig. 1 *a*). Arrow indicates the position of a 12.5-kb fragment in *l(3)dre3*^{rg35}*/TM6B* which is the result of the deletion removing the SalI site. The position of λHindIII digestion standards with their corresponding size is shown at left.

Phenotypic Analysis of α-Spectrin Mutants

Mutations in the *l(3)dre3* locus caused recessive zygotic lethality in the first instar of larval development with the exception of the *l(3)dre3*^{rg35} allele, which survived to second instar (Sliter et al. 1989). Examination of the *l(3)dre3* hemizygous or homozygous animals showed typical embryonic development. At the first instar stage the only noticeable consequence of spectrin deficiency was lethargic feeding behavior and sluggish movement prior to death. Upon dissecting these larvae, their gross anatomy appeared to be normal at the light microscope level; they possessed well-developed neuromuscular, respiratory and digestive tissues resembling their wild type counterparts at a similar stage of development.

We examined the subcellular localization of α-spectrin in *l(3)dre3*^{rg35} and *l(3)dre3*^{rg41} larvae, to determine if mislocalization or depletion of spectrin coincided with structural changes at the cellular level. Cells of digestive tissues were chosen for examination because of their large cell size. Changes in spectrin localization were evident in the gastric caeca region of the anterior midgut of *l(3)dre3*^{rg35} hemizygous larvae. In wild-type first instar larvae α-spectrin was associated with both the apical and basolateral plasma membrane of gastric caecal cells (Fig. 6 *a, arrows*), whereas in hemizygous *l(3)dre3*^{rg35} larvae, the distribution of α-spectrin was punctate and scattered throughout the cytoplasm of these cells, with reduced amounts of staining at the plasma membrane (Fig. 6 *b, arrows*). *l(3)dre3*^{rg41} homozygous larvae displayed a striking decrease in the staining of α-spectrin without the appearance of the punctate cytoplasmic staining seen in *l(3)dre3*^{rg35} larvae (Fig. 6 *c*). Since the antiserum does not recognize the first two segments of α-spectrin, we attributed the residual stain in limited regions of the basal surfaces of these cells (Fig. 6 *c, arrowheads*) to maternally provided spectrin. In conjunction with the loss of membrane-associated α-spectrin from the gastric caecal cells, there was a subtle change in the cellular architecture and overall tissue organization. Unlike gastric caeca of wild type animals (Fig. 6 *d*), the gastric caeca of *l(3)dre3*^{rg35} mutant larvae exhibited constrictions along their length (compare arrowed areas in Fig. 6, *d* and *e*). It is not known whether the shape changes occurred as a direct consequence of the loss of spectrin in gastric cells, or if loss of spectrin in surrounding smooth muscle cells produced muscle cells that were unable to restore gastric caecal cell shape after constriction. In addition, wild-type gastric caecal cells exhibited cytoplasmic granules that were normally restricted to the basal aspect of the cell (Fig. 6 *d, arrowheads*), but were scattered throughout the cytoplasm in *l(3)dre3*^{rg35} cells (Fig. 6 *e, arrowheads*).

The most noticeable structural change in the mutant larvae at the light microscope level was seen in the middle section of the midgut. The middle midgut is composed of an array of cuprophilic cells interspersed with interstitial cells. In wild-type larvae the apical perimeter of each cuprophilic cell forms an invaginated cup whose lumen is continuous with, and opens into, the gastric lumen through a pore (Fig. 7 *a, arrows*; Filshie et al., 1971). The prominent microvilli that line this cup, and the aperture (Fig. 7 *b, short arrows*) that is continuous with the lumen, are rich in F-actin as evident from phalloidin staining of these structures. Midgut cells of all the mutant larvae examined displayed a variety of structural aberrations, with their brush borders in disarray. Often the pore leading into the invaginations was splayed open and left the brush borders in direct contact with the midgut lumen, as is the case of the *l(3)dre3*^{rg41} larvae shown in Fig. 7 *c* (zone *1*). In some instances the brush borders showed extended pore structures (zone *2*), while in other regions, the general cup-shaped apical brush borders appeared to be intact (zone *3*).

α-spectrin staining in wild-type cuprophilic cells was localized to both the basolateral and apical cytoplasmic surfaces of the plasma membrane (Fig. 7 *d*). Because of the parasagittal plane of section in this confocal image (an example of which can be seen in the schematic, Fig. 7 *a*, cell furthest to the right), the basolateral surfaces of these cells appear to extend around the entire perimeter, giving the impression that the apical surface (Fig. 7 *d, arrowheads*) is enclosed by the basolateral surfaces (Fig. 7 *d, arrows*). In addition, the neighboring interstitial cells were not stained by the α-spectrin antibody. In cuprophilic cells of mutant *l(3)dre3*^{rg41} larvae of similar age, α-spectrin staining was absent from the apical surface and virtually undetectable in the basolateral domains (Fig. 7 *e*). Nomarski images comparing wild-type versus mutant midgut tissues also showed a derangement of the tissue and an absence of the brush border structures (compare Figs. 7, *f* and *g*). Furthermore, mutant midgut peritrophic membranes showed a propensity to be contorted (Fig. 7 *g*) rather than extended, as in the case of wild-type larvae (Fig. 7 *f*). Although starved wild-type larvae also displayed contorted peritrophic membranes, their cuprophilic cells, and specifically the brush borders, were structurally intact (data not shown).

Considering the localization of α-spectrin in wild-type cuprophilic cells one could argue that the loss of microvilli organization in spectrin deficient cells could either be due to

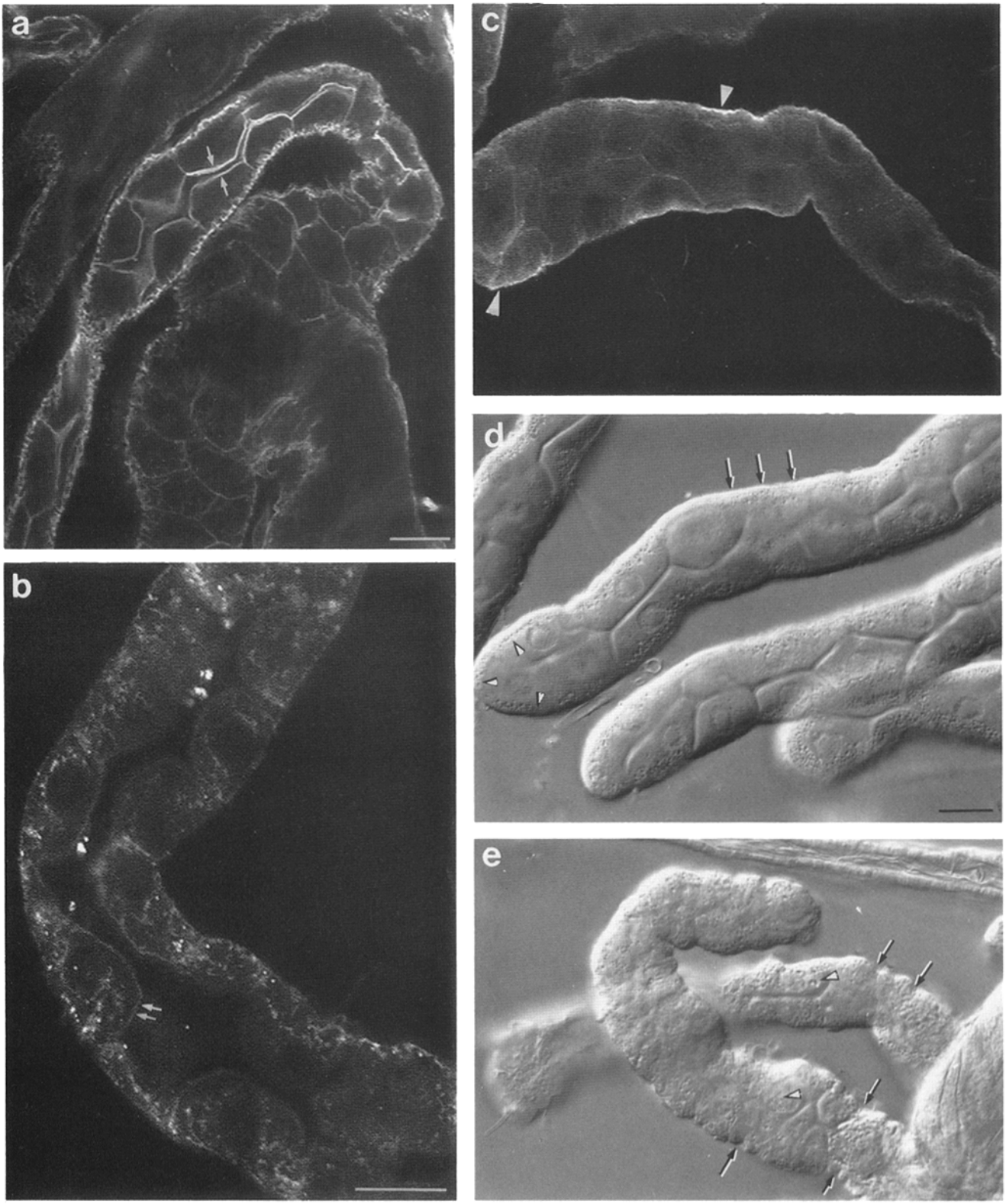

Figure 6. Distribution of α-spectrin in larval midgut. (*a*) Gastric caecal cells of first instar wild-type larvae show predominantly membrane-associated α-spectrin (*arrows*). (*b*) This distribution is perturbed in *l(3)dre3*^{rg35} tissues where the majority of spectrin is found in cytoplasmic aggregates and lesser amounts at the plasma membrane (*arrows*). (*c*) *l(3)dre3*^{rg41} tissues contain little α-spectrin except at some of the basal surfaces (*arrowheads*). (*d*) Nomarski photomicrograph of wild-type gastric caeca tissues with basolaterally restricted vesicles (*d*, *arrowheads*). (*e*) Mutant (*l(3)dre3*^{rg41}) gastric caeca tissue with vesicles throughout the cytoplasm at all focal planes examined; the mutant gastric caecal arms display constrictions along their lengths that are not found in wild-type tissues (compare arrowed regions in *d* and *e*). Bars, 10 μm.

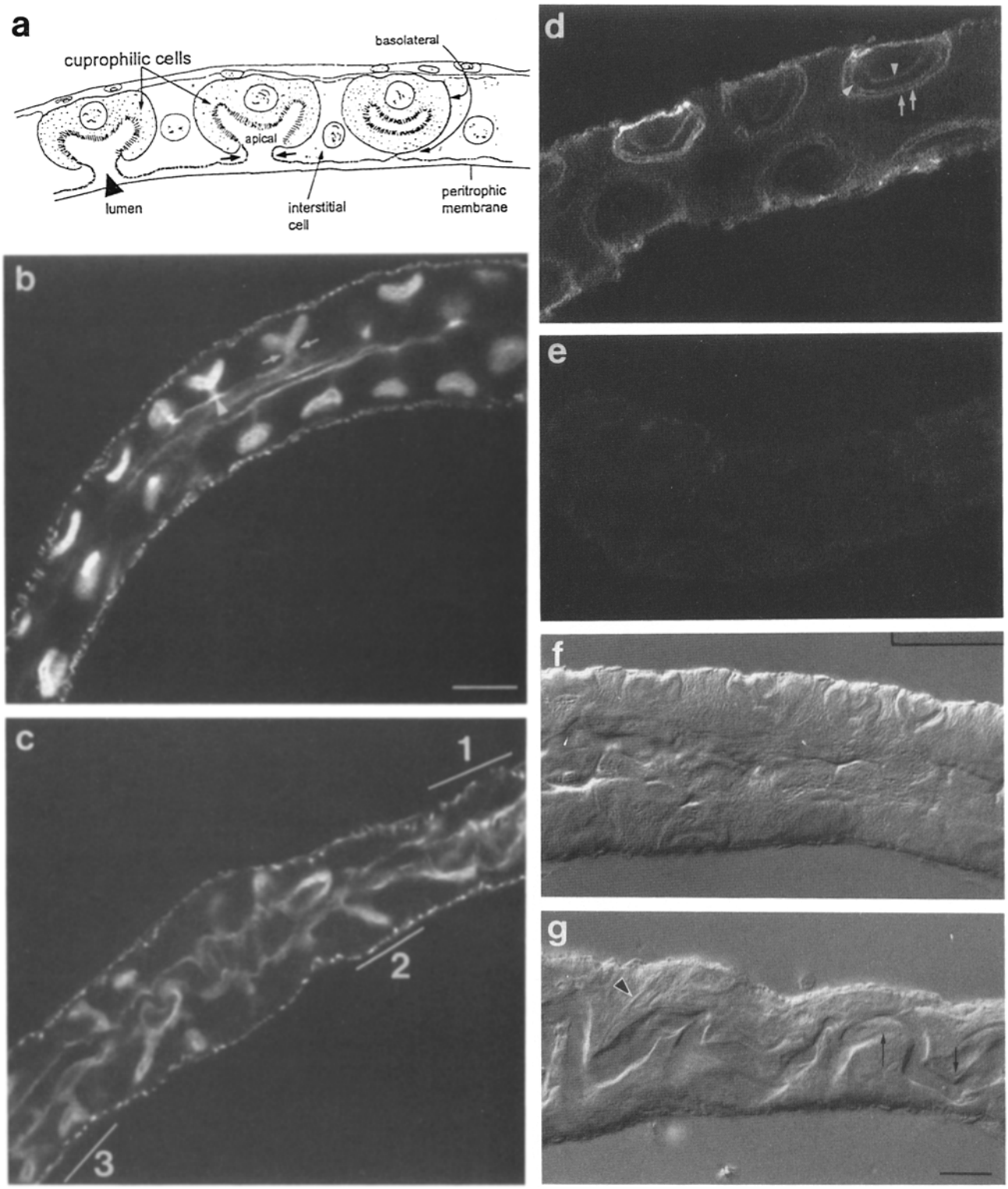

Figure 7. F-actin and α-spectrin distribution in copper-accumulating midgut cells. (*a*) Schematic of the middle midgut region of the *Drosophila* digestive system. Shown in longitudinal section are three cuprophilic cells separated by interstitial cells (Filshie et al., 1971). (*b*) Staining of wild-type midgut cell actin with TRITC-phalloidin demonstrates the regular cup-shaped array of brush borders in the cuprophilic cells. Short arrows in *a* and *b* point to the opening of the invaginated apical surface into the midgut lumen. (*c*) Midgut tissue from first instar *l(3)dre3*^{rg41} larvae display a range of disrupted brush border structures. The lines demark zones of different brush border morphologies (see Results). (*d* and *e*) Confocal sections of wild-type (*d*) and mutant (*e*) cuprophilic cells stained with α-spectrin antibody. α-spectrin is localized at the plasma membrane on the basolateral (*arrows*) as well as the apical surface (*arrowheads*) just underneath the brush border in wild-type cells. (*f* and *g*) Nomarski photomicrographs of wild-type (*f*) and mutant (*g*) midgut tissues. Mutant cuprophilic cells (*g*) show aberrant brush borders (*arrowhead*) as well as a contorted peritrophic membrane (*arrows*). Bar, 10 μm.

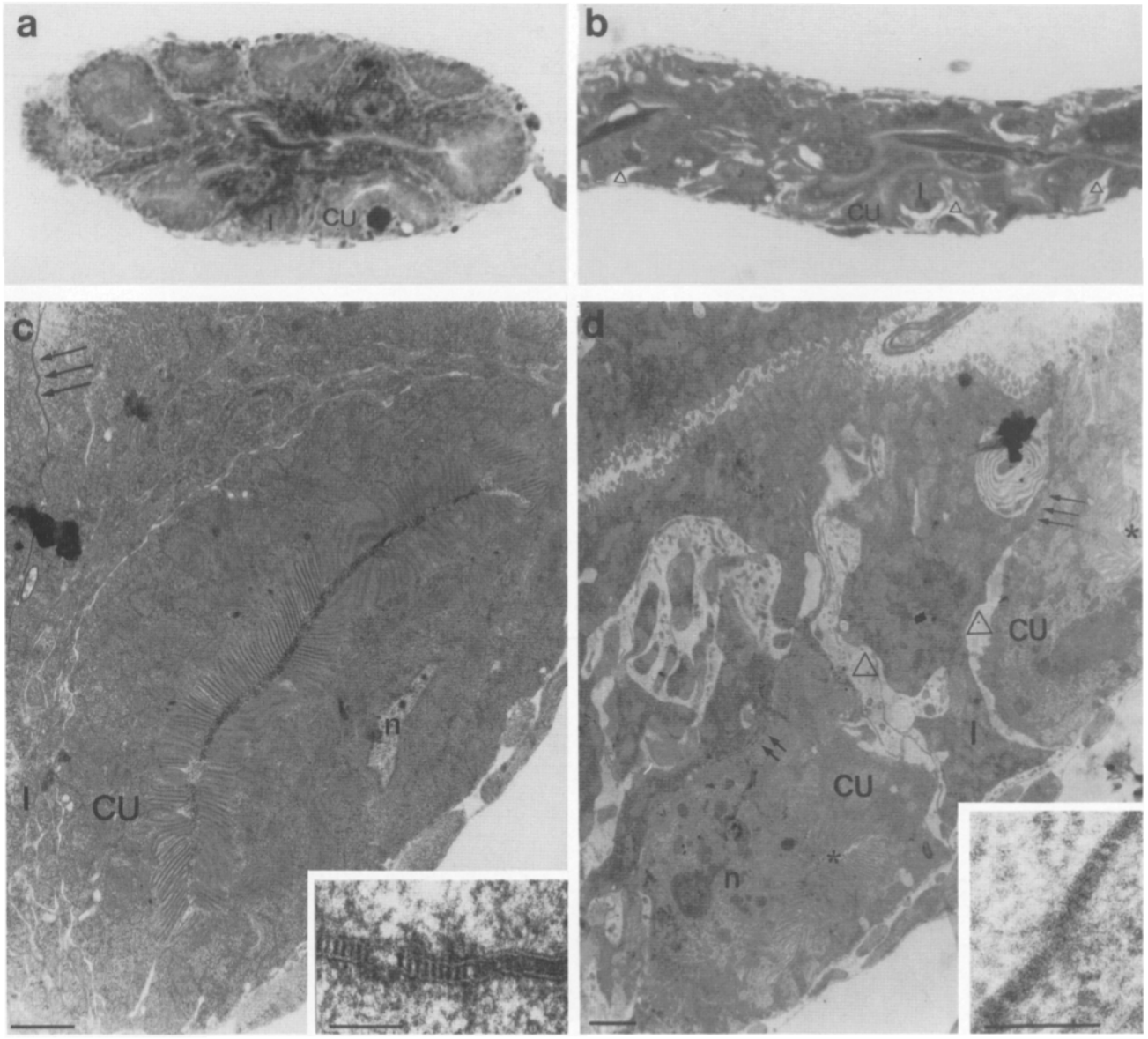

Figure 8. Ultrastructural analysis of middle midgut tissues. (*a* and *b*) Semi-thin sections of wild-type (*a*) and *l(3)dre3*^{rg41} mutant (*b*) tissues stained with methylene blue show the spatial relationship between cuprophilic (*CU*) and interstitial (*I*) cells. Open triangles (*b*) denote the intercellular spaces evident in mutant tissues. (*c* and *d*) Comparison of thin sections of wild-type (*c*) and mutant (*d*) tissues demonstrate the close membrane appositions between cuprophilic (*CU*) and interstitial cells (*I*) that are lost in α-spectrin deficient mutants (*triangles*). (*d*) Note the loss of cytoplasmic organization in the mutant cuprophilic cells (nuclei [*n*] is positioned apically). Electron-dense septate junctions (*c*, *arrows* and *inset*) are retained in the mutant cells (*d*, *arrows* and *inset*) despite the spectrin deficiency. Bars: (*c* and *d*) 1 μm; and (*insets*) 0.1 μm.

the loss of spectrin links between F-actin rootlets of the microvilli (Hirokawa et al., 1983) or a loss in cell adhesion that in turn influences cell shape and cytoplasmic organization. To distinguish between these two possibilities we examined both wild type (Fig. 8, *a* and *c*) and mutant (Fig. 8, *b* and *d*) midgut tissues at the ultrastructural level. Examination of mutant midgut tissues revealed large intercellular spaces between the interstitial and cuprophilic cells of *l(3)dre3*^{rg41} hemizygous larvae (Fig. 8 *b* and *d*, △). These sites of intercellular spaces replaced close membrane appositions between the plasma membrane of interstitial cells and the lateral aspect of the cuprophilic cells seen in wild-type tissues (Fig. 8 *c*). Interestingly, the septate junctions seen at the apices of the lateral membranes in wild-type tissues (Fig. 8 *c*, *arrows* and *inset*) remained largely intact in the α-spectrin–deficient cells (Fig. 8 *d*, *arrows* and *inset*). The loss of cell contact was accompanied by a loss of intracellular organization in the cuprophilic cells. In a number of mutant cuprophilic cells the nuclei were not in their usual basal position, rather they were apical relative to the brush border (Fig. 8 *d*). The microvilli of spectrin-deficient cells appeared to be intact but in some cases (Fig. 8 *d*, *asterisk*) lacked the closely packed organization seen in wild-type cells (Fig. 8 *b*). These structural differences account for the disrupted

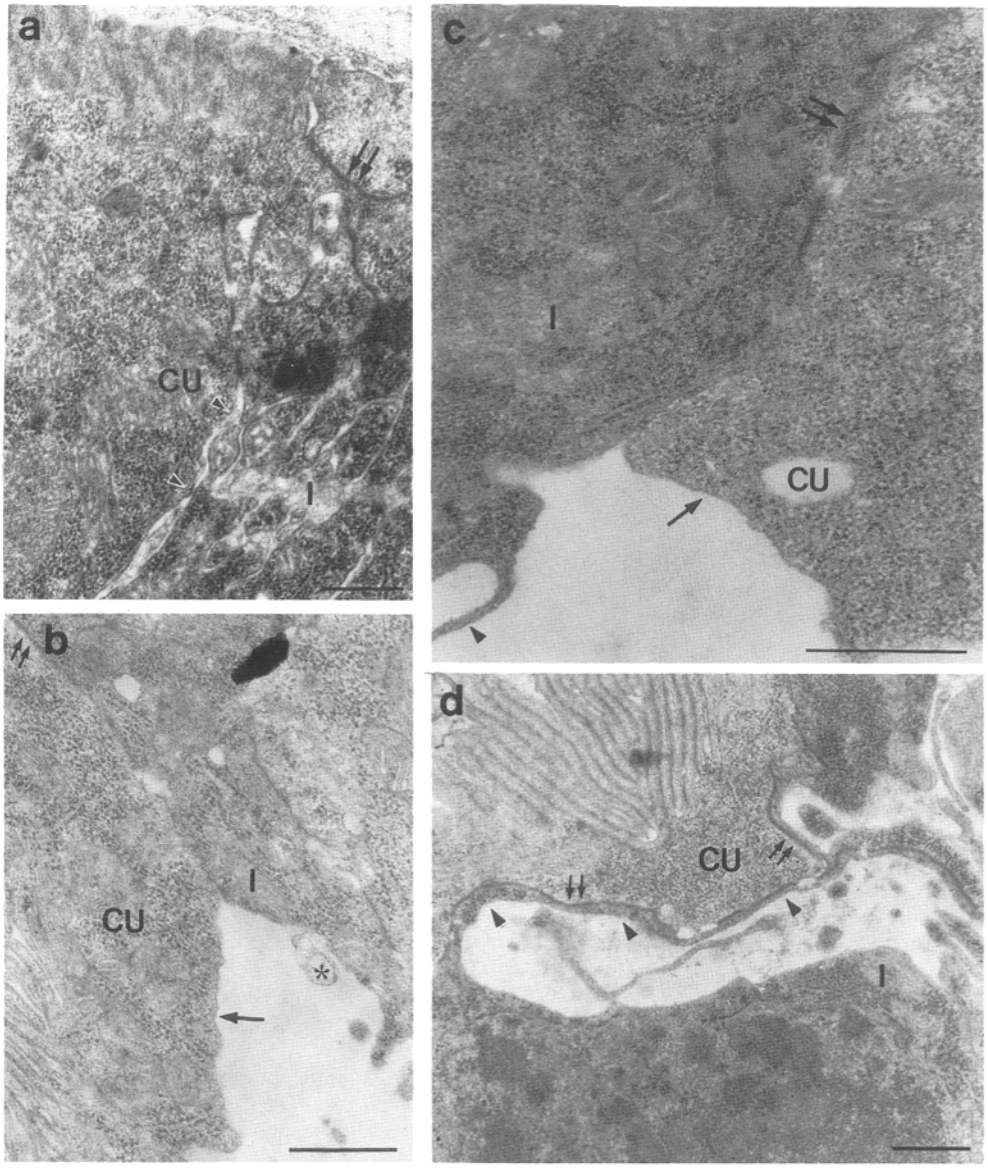

Figure 9. Electron micrographs of cuprophilic (*CU*) and interstitial (*I*) cell interactions. (*a*) Cell contacts of a wild-type larvae. Convoluted septate junctions (*double arrow*) gives way to close membrane appositions (*arrowheads*). (*b* through *d*) *l(3)dre3*^{rg41} mutant cells showing structures typical in mutant tissues. (*b*) Septate junction (*double arrow*) and plasma membrane of cuprophilic cell (*arrow*) appears to be intact whereas interstitial cell membrane is hard to resolve where a gap has formed between it and the cuprophilic cell. Myelin-like electron dense forms (*asterisk*) are seen associated with the interstitial cell. (*c*) Interstitial cell (*I*) shows a long extension of membrane (*arrowhead*). As in the previous panel cuprophilic cell membrane (*arrow*) is intact. (*d*) A septate junction region (*double arrows*) has retained a layer of interstitial cell membrane (*arrowheads*). Bars, 0.5 μm.

cellular arrangement seen in mutant midgut tissues by phalloidin staining. In addition, the loss of cell to cell contact was not restricted to the cuprophilic–interstitial cell contacts as cells along the entire digestive system displayed similar intercellular spaces that suggest a general loss of cell to cell interaction among epithelial cells of the gut (data not shown).

Closer examination of the cuprophilic and interstitial cell plasma membranes that separated from one another in the mutant tissues (Fig. 9) revealed that the plasma membranes of the cuprophilic cells appeared to be intact (Fig. 9, *b* and *c, arrows*) whereas the interstitial cell membranes exhibited structural alterations (despite not demonstrating detectable levels of α-spectrin staining in wild-type flies). Structural anomalies of interstitial cells included sloughing of myelin-like, electron-dense material (Fig. 9 *b, asterisk*) or long extensions of membrane (Fig. 9 *c, arrowhead*). Frequently, the intercellular spaces extended apically to the level of the septate junctions where the interstitial cell membrane and a layer of cell cytoplasm lined the junction interface with the cuprophilic cell (Fig. 9 *d, arrowheads*). Although we cannot exclude the possibility that some of these images were produced during fixation, they were not observed in wild-type cells and clearly suggest an instability in the interstitial cell plasma membrane or its immediately underlying cytoplasm.

In view of the postulated association of spectrin with Na^+,K^+-ATPase, (Nelson and Veshnock, 1987; and Morrow et al., 1989), we also examined the consequences of the α-spectrin deficiency on the polarized distribution of the ATPase in these cells. As expected (Amerogen et al., 1989) in wild-type cells that contained apical and basolateral spectrin (Fig. 10 *a*), the ATPase was restricted to the basolateral surface (Fig. 10 *b, arrows*). But, despite the loss of α-spectrin (Fig. 10 *c*) and consequent disrupted cell shape, cuprophilic cells of *l(3)dre3*^{rg41} homozygous larvae retained the basolateral distribution of Na^+,K^+-ATPase (Fig. 10 *d, arrows*).

Discussion

Our observations demonstrate that the *dre3* complementa-

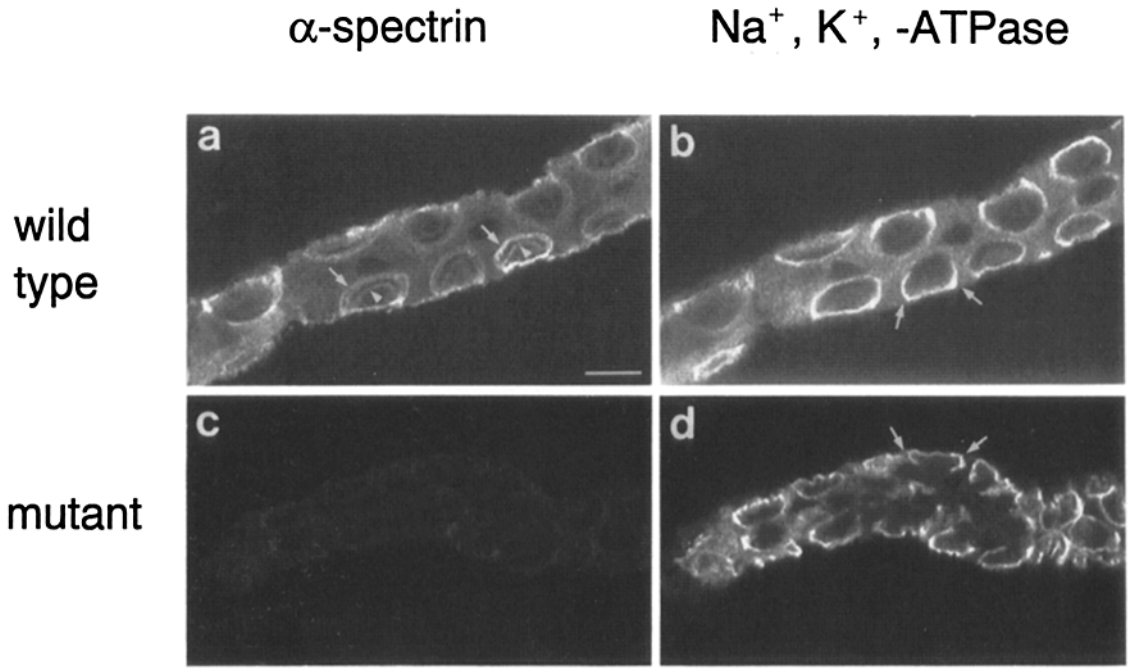

Figure 10. Distribution of α-spectrin and Na^+,K^+-ATPase in cuprophilic cells. Wild type (*a* and *b*) and mutant (*c* and *d*) cuprophilic cells doubly stained for both α-spectrin (*a* and *c*) and the α-subunit of ATPase (*b* and *d*). Wild-type (*l(3)dre3^{rg41}/TM6B*) midgut cells stained for α-spectrin (*a*) and Na^+,K^+-ATPase (*b*) show co-localization at the basolateral membrane (*arrows*) with additional α-spectrin staining at the apical surface (*a*, *arrowheads*). Similarly stained mutant cells (*l(3)dre3^{rg41}/Df(3L)R-R2*) display a lack of α-spectrin (*c*), disruption of cell shape, but retain Na^+,K^+-ATPase at the basolateral surface (*d*, *arrows*). Bar, 10 μm.

tion group in the *Dras-Roughened-ecdysoneless* region of chromosome 3 (Sliter et al., 1989) identifies the α-spectrin gene because germ line transformation with a wild-type α-spectrin minigene fully rescues these mutants. Furthermore, sequence analysis of the two γ-ray–induced alleles, *l(3)dre3^{rg35}* and *l(3)dre3^{rg41}*, showed deletions within the α-spectrin coding sequence. These deletions result in frameshifts and premature termination that produced null mutants or mutants with truncated products. All the alleles in the *dre3* group (generated by both γ-ray and EMS-mutagenesis) produced recessive zygotic lethality at either the first or second instar stage of larval development (Sliter et al. 1989). Pesacreta et al. (1989) have reported that a large pool of α-spectrin is provided to embryos maternally. Our results suggest that mutant larvae use this maternal spectrin to complete embryogenesis, but without zygotic expression of α-spectrin, newly hatched larvae do not develop beyond first instar. Thus, although the depletion of spectrin in tissue culture cells did not present an obvious phenotype (Mangeat and Burridge, 1984), the analysis of *Drosophila* α-spectrin mutants indicates a requirement for α-spectrin in structural aspects of fly development.

Since spectrin is a ubiquitously expressed protein, its deficiency is presumed to affect a variety of tissues on a time scale dependent on turnover of maternal α-spectrin (which may differ from tissue to tissue). In the case of the midgut cuprophilic cells, it is not until after hatching that mutant larvae begin to show loss of cell contact and deranged brush borders. Based on the electron micrographs, we conclude that as spectrin is depleted, loss of cell to cell contact leads to the deranged brush border phenotype. It may be argued that loss of α-spectrin itself affects cell shape creating intercellular gaps to the extent seen in mutant midgut tissues. But this does not seem likely since the interstitial cells, which we find do not contain a detectable α-spectrin–based membrane skeleton, undergo as significant a change in cell shape as do the cuprophilic cells which contain a spectrin membrane skeleton. Rather, we argue that the depletion of an α-spectrin-based membrane skeleton influences the proper placement of molecules involved in the adhesion of the two cell types. A similar situation may hold in the salivary glands of α-spectrin deficient mutants, where we have observed a homogeneous population of cells affected in their ability to retain contact (not shown). Support for the notion that spectrin influences the placement of extracellular adhesion molecules is provided by the observations that cell to cell contacts in mammals involve a complex between basolateral spectrin, ankyrin and the adhesion protein, uvomorulin (Nelson et al., 1990). Verifying this hypothesis requires that the adhesion molecules of the fly gut epithelium be defined, and their interactions, if any, with a spectrin-based membrane skeleton be characterized.

The spectrin-based membrane skeleton has been proposed to play a role in establishing and maintaining the polarity of integral membrane proteins such as Na^+,K^+-ATPase (Nelson and Veshnock, 1987; Morrow et al., 1989). Given the perdurance of maternal spectrin beyond the developmental stage at which midgut cells form, the consequences of the *l(3)dre3^{rg41}* spectrin mutation on the *establishment* of membrane polarity cannot be rigorously resolved at present. But, our observation that Na^+K^+-ATPase is retained at the basolateral plasma membranes of spectrin-deficient midgut cells suggests that the continued *maintenance* of the basolateral polarity of Na^+K^+-ATPase does not solely depend upon an

α-spectrin–based membrane skeleton. Rather, retention of basolateral polarity could be due to a "barrier" provided by the septate junctions that we have observed to be maintained in α-spectrin–deficient cells. On the other hand, we cannot rule out the possibility (Hammerton et al., 1991) that the time required to clear sufficient ATPase from the basolateral surface to detect a loss of signal by immunofluorescence may be longer than the time between depletion of maternal spectrin and the subsequent death of these larvae.

Our examination of the *l(3)dre3*^{rg35} allele provides new insight into the importance of α-spectrin's second EF hand that is missing in this mutant. Although the truncated spectrin produced by *l(3)dre3*^{rg35} allowed this mutant to survive through first instar development, loss of the second EF hand in the truncated α-spectrin synthesized by *l(3)dre3*^{rg35} was nevertheless lethal in second instar. Survival to second instar may reflect the ability of the *l(3)dre3*^{rg35} product to prolong the half-life of the β-spectrin subunit in at least some tissues of the developing larvae. This idea is consistent with the finding that the interchain binding site on the α-subunit is located within repeat segments 19-21 and does not require the EF hands themselves (Speicher et al., 1992).

The observation that spectrin localizes in cytoplasmic aggregates in gastric caecal cells of *l(3)dre3*^{rg35} larvae (Fig. 6) suggests that the ability of the truncated product to target the plasma membrane of these cells is disrupted when the last 90–amino acid residues of α-spectrin are missing. Preliminary results using heterodimers formed between the truncated α-spectrin of the *l(3)dre3*^{rg35} allele and wild-type β-spectrin indicates that actin-binding activity is not inhibited by the *l(3)dre3*^{rg35} product (data not shown). To what degree actin-binding activity in vivo is affected by the altered heterodimers is not known. The loss of the second EF hand may eliminate a potential regulatory function of Ca^{2+} on the interaction between the spectrin heterodimer and actin filaments in the cells that is not detected by the in vitro assay. Failure to regulate actin binding may, in turn, be related to the mislocalization of α-spectrin in these cells.

While our observation that cell to cell contacts are lost in epithelial cells of the gut in α-spectrin mutants supports the general view that spectrin and related proteins (α-actinin and dystrophin) stabilize regions of cell to cell contact (Sobel and Alliegro, 1985; Shatten et al., 1986; Pesacreta et al., 1989; Stedman et al., 1991; Roulier et al., 1992), direct experimental evidence for these notions requires more detailed information about the cell surface molecules that are involved. Experiments that correlate the in vitro and in vivo effects of alterations in selected and limited regions of the spectrin molecule will be required for a molecular understanding of the developmental and morphological aberrations evident in spectrin mutants. Our characterization of the *l(3)dre3* alleles as spectrin mutants now make such experiments possible.

We thank the members of the Branton and Goldstein laboratories for helpful discussions during the course of this work. We are grateful to Lawrence Gilbert for providing stocks of the *dre* complementation groups, to Mike Caplan for the gift of the anti-Na^+K^+-ATPase antibody, and to John Lis for the ubiquitin clone. We thank Chris Lee for the initial round of screening for the genomic α-spectrin clones.

This work was supported by National Institutes of Health grant GM 39686 to D. Branton. J. Lee and R. Dubreuil were supported by postdoctoral fellowships from the American Cancer Society.

Received for publication 30 March 1993 and in revised form 11 October 1993.

References

Amerogen, H. M., J. A. Mack, J. M. Wilson, and M. R. Neutra. 1989. Membrane domains of intestinal epithelial cells: distribution of Na^+,K^+-ATPase and the membrane skeleton in adult rat intestine during fetal development and after epithelial isolation. *J. Cell Biol.* 109:2129–2138.

Bennett, V. 1990. Spectrin-based membrane skeleton: a multipotential adaptor between plasma membrane and cytoplasm. *Physiol. Rev.* 70:1029–1065.

Brehme, K. S. 1941. The effect of adult body color mutations upon the larva of *Drosophila melanogaster*. *Proc. Natl. Acad. Sci. (USA).* 27:254–261.

Burnette, W. N. 1981. Electrophoretic transfer of proteins from sodium dodecyl sulfate-polyacrylamide gels to unmodified nitrocellulose and radiographic detection with antibody and radioiodinated protein A. *Anal. Biochem.* 112:195–203.

Byers, T. J., R. R. Dubreuil, D. Branton, D. P. Kiehart, and L. S. B. Goldstein. 1987. *Drosophila* spectrin. II. Conserved features of the alpha-subunit are revealed by analysis of cDNA clones and fusion proteins. *J. Cell Biol.* 105:2103–2110.

Byers, T. J., E. Brandin, R. A. Lue, E. Winograd, and D. Branton. 1992. The complete sequence of *Drosophila* β-spectrin reveals supra-motifs comprising eight 106-residue segments. *Proc. Natl. Acad. Sci. (USA).* 89:6187–6191.

Casanova, J. L., C. Pannetier, C. Jaulin, and P. Kourilsky. 1990. Optimal conditions for directly sequencing double-stranded PCR products with Sequenase. *Nucleic Acids Res.* 18:1028.

Church, G., and W. Gilbert. 1984. Genomic sequencing. *Proc. Natl. Acad. Sci. (USA).* 81:1991–1995.

Cooley, L., R. Kelley, and A. Spradling. 1988. Insertional mutagenesis of the *Drosophila* genome with single P-elements. *Science (Wash. DC).* 239: 1121–1128.

Coyne, R. S. 1989. Molecular and genetic analysis of the *Drosophila* α-spectrin region. Ph.D. Thesis. Harvard University. 206 pp.

Davies, K. A., and S. E. Lux. 1989. Hereditary disorders of the red cell membrane skeleton. *Trends Genetics.* 5:222–227.

Dubreuil, R. R., T. J. Byers, D. Branton, L. S. B. Goldstein, and D. P. Kiehart. 1987. *Drosophila* spectrin. I. Characterization of the purified protein. *J. Cell Biol.* 105:2095–2102.

Dubreuil, R. R., T. J. Byers, A. L. Sillman, D. Bar-Zivi, L. S. B. Goldstein, and D. Branton. 1989. The complete sequence of *Drosophila* α-spectrin: conservation of structural domains between α-spectrins and α-actinin. *J. Cell Biol.* 109:2197–2205.

Dubreuil, R. R., E. Brandin, J. H. Sun Reisberg, L. S. B. Goldstein, and D. Branton. 1991. Structure, calmodulin-binding, and calcium-binding properties of recombinant α-spectrin polypeptides. *J. Biol. Chem.* 266:7189–7193.

Feinberg, A. P. and B. Vogelstein. 1983. A technique for radiolabelling DNA restriction endonuclease fragments to high specific activity. *Anal. Biochem.* 132:6–13.

Filshie, D. K., D. F. Poulson, and D. F. Waterhouse. 1971. Ultrastructure of the copper-accumulating region of the *Drosophila* larval midgut. *Tissue & Cell.* 3:77–102.

Fowler, V. M., and E. J. H. Adam. 1992. Spectrin redistributes to the cytosol and is phosphorylated during mitosis in cultured cells. *J. Cell Biol.* 119: 1559–1572.

Hammerton, R. W., K. A. Krzeminski, R. W. Mays, T. A. Ryan, D. A. Wollner, and W. J. Nelson. 1991. Mechanism for regulating cell surface distribution of Na^+,K^+-ATPase in polarized epithelial cells. *Science (Wash. DC).* 254:847–850.

Hirokawa, N., R. E. Cheney, and M. Willard. 1983. Location of a protein of the fodrin-spectrin-TW260/240 family in the mouse intestinal brush border. *Cell.* 32:953–965.

Klemenz, R., U. Weber, and W. J. Gehring. 1987. The white gene as a marker in a new P-element vector for gene transfer in *Drosophila*. *Nucleic Acids Res.* 15:3947–3959.

Laemmli, U. K. 1970. Cleavage of structural proteins during the assembly of the head of bacteriophage T4. *Nature (Lond.).* 227:680–685.

Lebovitz, R. M., K. Takeyasu, and D. M.Fambrough. 1989. Molecular characterization and expression of the Na^+,K^+-ATPase α-subunit in *Drosophila melanogaster*. *EMBO (Eur. Mol. Biol. Organ.) J.* 8:193–202.

Lee, H. S., J. A. Simon, and J. T. Lis. 1988*a*. Structure and expression of ubiquitin genes of *Drosophila melanogaster*. *Mol. Cell. Biol.* 8:4727–4735.

Lee, J. K., J. D. Black, E. A. Repasky, R. T. Kubo, and R. B. Bankert. 1988*b*. Activation induces a rapid reorganization of spectrin in lymphocytes. *Cell.* 55:807–816.

Lindsley, D. L., and G. G. Zimm. 1992. The genome of *Drosophila melanogaster*. Academic Press, San Diego, CA. 1,133 pp.

Mangeat, P. H., and K. Burridge. 1984. Immunoprecipitation of nonerythrocyte spectrin within live cells following microinjection of specific an-

tibodies: relation to cytoskeletal structures. *J. Cell Biol.* 98:1363–1377.
Mercier, F., H. Reggio, G. Devilliers, D. Bataille, and P. H. Mangeat. 1989. Membrane-cytoskeleton dynamics in rat parietal cells: mobilization of actin and spectrin upon stimulation of gastric acid secretion. *J. Cell Biol.* 108:441–453.
Morrow, J. S., S. D. Ciani, T. Ardito, A. S. Mann, and M. Kashgarian. 1989. Ankyrin links fodrin to α-subunit of Na^+,K^+-ATPase in Madin-Darby canine kidney cells and in intact renal tubule cells. *J. Cell Biol.* 108:455–465.
Nelson, W. J., and P. J. Veshnock. 1987. Ankyrin binding to Na^+,K^+-ATPase and implications for the organization of membrane domains in polarized cells. *Nature (Lond.).* 328:533–536.
Nelson, W. J., E. M. Shore, A. Z. Wang, and R. W. Hammerton. 1990. Identification of a membrane-cytoskeletal complex containing the cell adhesion molecule uvomorulin (E-cadherin), ankyrin, and fodrin in Madin-Darby canine kidney epithelial cells. *J. Cell Biol.* 110:349–357.
Palek, J. and S. Lambert. 1990. Genetics of the red cell membrane skeleton. *Semin. Hematol.* 27:290–332.
Pesacreta, T. C., T. J. Byers, R. Dubreuil, D. P. Kiehart, and D. Branton. 1989. *Drosophila* spectrin: the membrane skeleton during embryogenesis. *J. Cell Biol.* 108:1697–1709.
Reed, K. C., and D. A. Mann. 1985. Rapid transfer of DNA from agarose gels to nylon membranes. *Nucleic Acids Res.* 7207–7221.
Robertson, H. M., C. R. Preston, R. W. Philips, D. M. Johnson-Shlitz, W. K. Benz, and W. R. Engels. 1988. A stable source of *P* element transposase in *Drosophila melanogaster*. *Genetics.* 118:461–470.
Roulier, E. M., C. Fyrberg, and E. Fyrberg. 1992. Perturbation of *Drosophila* α-actinin causes muscle paralysis, weakness, and atrophy but do not confer obvious nonmuscle phenotypes. *J. Cell Biol.* 116:911–922.
Saiki, R. K., D. H. Gelfand, S. Stoffel, S. J. Scharf, R. Higuchi, G. T. Horn, K. B. Mullis, and H. A. Erlich. 1988. Primer-directed enzymatic amplification of DNA with a thermostable DNA polymerase. *Science (Wash. DC).* 239:487–491.
Shatten, H., R. Cheney, R. Balczon, M. Willard, C. Cline, C. Simerly, and G. Shatten. 1986. Localization of fodrin during fertilization and early development of sea urchins and mice. *Dev. Biol.* 118:457–466.
Simon, J. A., C. A. Sutton, R. B. Lobell, R. L. Glaser, and J. T. Lis. 1985. Determinants of heat shock-induced chromosome puffing. *Cell.* 40:805–817.
Sliter, T. J., V. C. Henrich, R. L. Tucker, and L. I. Gilbert. 1989. The genetics of the *Dras-Roughened-ecdysoneless* chromosomal region (62B3-4 to 62D3-4) in *Drosophila melanogaster*: Analysis of recessive lethal mutations. *Genetics.* 123:327–336.
Sobel, J. S., and M. A. Alliegro. 1985. Changes in the distribution of a spectrin-like protein during development of the preimplantation mouse mebryo. *J. Cell Biol.* 100:333–336.
Speicher, D. W., L. Weglarz, and T. M. DeSilva. 1992. Properties of human red cell spectrin heterodimer (side by side) assembly and identification of an essential nucleation site. *J. Biol. Chem.* 267:14775–14782.
Spradling, A. C. and G. M. Rubin. 1982. Transposition of cloned *P* elements into *Drosophila* germ line chromosomes. *Science (Wash. DC).* 218: 341–347.
Stedman, H. H., H. L. Sweeney, J. B. Shrager, H. C. Maguire, R. A. Panettieri, B. Petrof, M. Narusawa, J. M. Leferovich, J. T. Sladky, and A. M. Kelly. 1991. The *mdx* mouse diaphragm reproduces the degenerative changes of Duchenne muscular dystrophy. *Nature (Lond.).* 352:536–539.
Theurkauf, W. E. 1992. Behavior of a structurally divergent α-tubulin isotype during *Drosòphila* embryogenesis: evidence for post-translational regulation of isotype abundance. *Dev. Biol.* 154:205–217.
Winograd, E., D. Hume, and D. Branton. 1991. Phasing the conformation unit of spectrin. *Proc. Natl. Acad. Sci. (USA).* 88:10788–10791.